Accepted Manuscript

Scottish Journal of Geology

Trace and minor element concentrations in sulfide ore material from the Leadhills and Wanlockhead orefield, SW Scotland

David Currie, Andie Bryce, Neil Burnside, Hannah Grant & Lauren Tuffield

DOI: https://doi.org/10.1144/sjg2025-010

To access the most recent version of this article, please click the DOI URL in the line above. When citing this article please include the above DOI.

This article is part of the Scottish Journal of Geology Collection on Early-Career Research collection available at: https://www.lyellcollection.org/topic/collections/early-career-research

Received 29 May 2025
Revised 25 September 2025
Accepted 21 October 2025

Supplementary material at https://doi.org/10.6084/m9.figshare.c.8285652

Title: Trace and minor element concentrations in sulfide ore material from the Leadhills and Wanlockhead orefield, SW Scotland

Abbreviated title: Trace elements in base metal sulfides from SW Scotland

David Currie[1,*], Andie Bryce[2], Neil Burnside[2], Hannah Grant[1], Lauren Tuffield[1]

[1] British Geological Survey, Keyworth, Nottinghamshire, NG125GG

[2] University of Strathclyde, 16 Richmond St, Glasgow G1 1XQ

* Correspondence: dcur@bgs.ac.uk ORCID: 0009-0006-3460-5253

Abstract

Building on a knowledge-based prospectivity analysis conducted by the BGS in 2023, this study assessed the potential for sphalerite, galena, chalcopyrite, and pyrite from the Leadhills and Wanlockhead orefield (LWO), Southwest Scotland to host critical minerals.

Utilising SEM and LA-ICP-MS, sphalerite was found to be the primary host for Ga, Ge and Ag, while chalcopyrite was identified as the primary host for In, Se, and Sn, and galena the primary host for Sb. For sphalerite, the geometric mean concentration of Ge was 200 ppm with a maximum value of 860 ppm. These values indicate significant enrichment of Ge in sphalerite relative to crustal abundances and are comparable to significant Ge-producing deposits like Red Dog, Alaska, and the formerly productive Noailhac-Saint Salvy deposit in France.

Cadmium, Se, and As were found to be hosted by sphalerite, chalcopyrite, and pyrite respectively. These elements are known to have detrimental effects on human health and ecological and environmental systems. A further orefield-wide assessment of mine waste material to fully document the occurrence of sphalerite in veins and mine waste is recommended.

Introduction

In mining, primary products are the main raw minerals or metals extracted from an ore, such as construction, industrial, and energy minerals or metals like Cu, Au, or Fe. Co-products are additional valuable minerals or metals that are extracted from the same ore material, each with substantial economic value, like Ag from Pb and Zn processing. By-products are secondary materials recovered during the extraction of primary products, such as Co from Cu Ni mining, or In and Ge from Zn refining. These by-products, often accounting for less

than 0.1 per cent of an ore material, have become essential components in many high-tech and decarbonisation technologies such as telecommunications, renewable energy, electric vehicles, aerospace, medical, agriculture, and defence sectors (Nassar et al., 2015).

The demand for these by-products is expected to grow significantly due to rising global populations and the push for low-carbon technologies (International Energy Association, 2025). In the context of this study, it is worth noting that the concentration of trace elements in a primary ore is very similar to that of by-products but that not all trace-elements are recoverable as by-products since their economic viability and feasibility of extraction must be considered.

Although no single country is entirely self-sufficient in terms of producing and refining all raw materials and processed products needed to sustain modern industrial sectors, several countries do hold significant capacity to either produce the raw materials or refine the raw materials to create the processed product (Mudd et al., 2024). This creates a multitude of risks, for both the exporting country and importing countries. Supply risks caused by wars, tariffs, export restrictions, and environmental disasters may lead to challenges across that commodities supply chain. Relying on a single commodity to form the backbone of a country's economy can also lead to acute challenges for that country if any import, production and/or export issues occur, too.

For many countries globally, the by-product materials account for the majority of the elements and raw materials now deemed to be either 'critical' or 'strategic' or are monitored on national 'watchlists' (Mudd et al., 2024). Consequently, understanding the geological, geochemical, and metallurgical relationships between primary, co- and by-products of national resources can increase the likelihood of diversifying future by-product availability in material markets and create more secure supply chains of these materials going forward. Moreover, the reprocessing of mine waste and tailings from historic mining sites may be a route to securing a more stable supply of by-products and revitalising communities affected by mine closures, whilst also reducing environmental and societal risks associated with mining (Vitti and Arnold, 2022, Lottermoser, 2011, Moyo et al., 2023).

Studies focussing on trace elements in sulfide ores have been ongoing since the pioneering work of de Boisbaudran (1875) which led to the discovery of Ga in sphalerite; an overview of these early studies is provided by Fleischer (1955). Since the advent of more sophisticated microanalytical techniques, like laser-ablation inductively-coupled plasma mass spectrometry (LA-ICP-MS), an ever-increasing amount of trace element data related to base

metal sulfides has become openly available (Cook et al., 2009, George et al., 2016, Frenzel et al., 2016, Huston and Bastrakov, 2024 and references therein). This type of compositional data is typically used to better understand the optimal geological and physiochemical conditions under which these trace elements partition into base metal sulfides; a review and meta-analysis is provided by Frenzel et al. (2016).

For example, lower temperature sphalerite mineralisation is more likely to incorporate Ga and Ge whereas In is more likely to be partitioned into sphalerite at higher temperatures (Frenzel et al., 2016). More recent studies have noted the physiochemical conditions preferable for trace element enrichment in base metal sulfides and have applied them to data- and knowledge-driven mineral systems approaches for prospectivity analysis (e.g. Huston and Bastrakov, 2024; Deady et al., 2023). The mineral system approach is now widely used in ore exploration and can recognise geological occurrences and/or regions historically deemed barren or unconventional (McCuaig et al., 2010, Barnes et al., 2016, Huston and Bastrakov, 2024, Groves et al., 2020).

The Leadhills and Wanlockhead Orefield (LWO), located around Scotland's highest village of Wanlockhead and neighbouring Leadhills, was recently identified through a knowledge-driven mineral systems approach as being potentially prospective for Ga, Ge, and In (Deady et al., 2023). This was based on the extensive historic mining of Pb-Zn ± (Cu-Ag)-rich low temperature epithermal veins across the area. In the most recent criticality assessment for the UK, Ga, Ge, In, and Zn were identified as being critical minerals (Mudd et al., 2024).

However, the LWO has also been subject to negative environmental reports. Levels of Fe, Pb, Zn, As, Cd, and Cu in the mine run-off and stream water, and Pb, Fe, Mg, Cu, Zn, and Mn in the historic spoil heaps exceed UK Environmental Quality Standards (EQS) (Byrne and Yendell, 2020) and fail to meet the Water Framework Directive's requirements (Chukwura and Hursthouse, 2020).

The following section gives brief insight into the main sulfide ore minerals present in veins and the spoil heaps and tailings across the LWO. Sphalerite (ZnS) is the main ore of Zn and is found in various geological settings globally such as sediment hosted massive sulfide deposits (SHMS), Mississippi Valley type (MVT), and volcanogenic massive sulfide (VMS) deposits (Frenzel et al., 2016, Huston and Bastrakov, 2024). Its colour varies from light to dark brown, red, yellow, green, and black, depending on its Fe, Mn, and Co content (Cook et al., 2009). Sphalerite can also contain trace through to significant amounts of other elements like Cu, Cd, Ga, Ge, and In, which in economic quantities may be extracted during refining

(Cook et al., 2009). For example, sphalerite from the epithermal precious- and base-metal veins of Farallón Negro Mining District, northwestern Argentina are known to contain over 24 wt% In and 13 wt% Cu, but are still classed as sphalerite (Márquez-Zavalía et al., 2024)

Galena (PbS) is the primary ore of Pb, characterised by its cubic habit, lead-grey colour, and metallic to sub-metallic lustre. It is commonly found in hydrothermal veins and often associated with sphalerite, chalcopyrite, and pyrite. Galena can contain significant amounts of Ag, Sb, and Bi which can be extracted during refining (George et al., 2015, Zhou et al., 2023).

Chalcopyrite ($CuFeS_2$) is the most abundant Cu ore mineral, with a brassy to golden yellow colour and metallic lustre. It is found in various sulfide mineral deposits globally, most prominently in porphyry Cu or stratiform sedimentary hosted deposits (Cailteux et al., 2005, Sillitoe, 2010). Chalcopyrite can also contain Au, Se, Te, Mo, Re, Co, In, Ge, and Sn, which can be extracted during refining (Moats et al., 2021, Ayres et al., 2013).

Pyrite (FeS_2) is found in a wide range of ore deposits and has a pale brass-yellow colour and metallic lustre, forming cubic or octahedral crystals. It is often associated with other sulfide minerals like chalcopyrite, sphalerite, and galena. While not a primary ore of Fe, pyrite is sometimes mined for its sulfur content and as a source of sulfuric acid and Au (Cook et al., 2013, Oliveira et al., 2012). Pyrite can also contain significant amounts of Co, Ni, As, Ag, Te, Au and Se (Cook et al., 2013). The association between pyrite and Au is most notable in Carlin-type Au deposits (Large et al., 2009).

In this study we characterise sphalerite, galena, chalcopyrite, and pyrite mineralisation from veins across the LWO using scanning electron microscopy (SEM) and energy dispersive X-ray analysis (EDX) and, for the first time, LA-ICP-MS analysis of these sulfides to provide quantitative minor and trace element data. The data collected here are subsequently compared to a global dataset of trace element concentrations in similar sulfide ores and are discussed in the context of environmental risk and future research and resource potential.

Regional geology

The LWO is located within the Southern Upland Terrane (SUT), which spans approximately 10,000 km² in southern Scotland and around 6,000 km² in the Longford-Down Massif of Northern Ireland and the Republic of Ireland.

This terrane is an accretionary complex formed during the Caledonian Orogeny, characterised by Ordovician and Silurian turbidite successions composed of greywacke sandstones, siltstones, and mudstones (McKerrow et al., 1977; Leggett et al., 1979; Stone, 2014).

The SUT comprises NE-SW striking, steeply dipping, folded, and low-grade metamorphosed formations with distinct detrital mineralogy (Kemp and Merriman, 2001). For instance, the Portpatrick Formation, which hosts the LWO, contains clasts of hornblende-andesite, gabbro, diorite, and glaucophane schist (Mange et al., 2005; British Geological Survey, 1993). This formation is relatively more calcic than other SUT units, with elevated TiO_2, Cr, and Ni levels suggesting a more evolved mafic and ophiolitic source. These formations are separated by high-angle thrust faults, often associated with interbedded black shales, siliceous mudstones, extrusive igneous assemblages, and cherts (Stone, 2014).

Igneous bodies across the SUT range from the late Cambrian to Ordovician Ballantrae Complex to Devonian andesitic lavas and Palaeogene dykes (Hines et al., 2018; Miles et al., 2014; Gemmell et al., 2025). Notable post-tectonic Siluro-Devonian granites include Loch Doon, Cairnsmore of Carsphairn, Cairnsmore of Fleet, Criffel-Dalbeattie, and Tweeddale. Two late Silurian–Devonian intrusive bodies—the Ballencleuch Law granite and the Spango pluton granodiorite—are located near the LWO (Pickett and Floyd, 2003). Additionally, felsic intrusive bodies, locally referred to as ‘felsites,’ crop out adjacent to vein mineralisation and cut through greywacke sandstone, shales, and cherts in the LWO area (Pickett and Floyd, 2003).

Transtensional reactivation of NE-SW Caledonian structures from the Devonian period onward led to NW-SE trending Lower Devonian to Triassic basins across the SUT (Stone, 2014). Palaeozoic fluviatile and aeolian sediments were deposited unconformably over steeply dipping Silurian strata. A conformable transition from continental to marine sedimentation is recorded across several basins, with limestone and Yoredale cyclothem deposition overlying Lower Palaeozoic strata (Pickett and Floyd, 2003).

In Upper Nithsdale and Canonbie, these sequences are overlain by productive Carboniferous Coal Measures. However, in the Thornhill Basin, located a few kilometres south of the LWO, the coal measures are intensely weathered and unproductive (McMillan and Brand, 1995). The role of these basins in supplying fluids and metals for ore mineralisation at LWO remains uncertain.

A pulse of early Cenozoic denudation, coupled with several subsequent glacial cycles, has led to the removal of approximately 1.2 km of rock across the SUT. The LWO likely experienced less erosion, having remained a prominent high point during glacial periods (Łuszczak et al., 2018).

Historic and geological context for the Leadhills and Wanlockhead Orefield

Mining activities potentially dating back to the medieval period—or perhaps even the Late Bronze and Iron Ages—have been identified through atmospheric metal contamination in peat bog cores surrounding the LWO (Mighall et al., 2014). The first documented mining across the LWO dates to the 13th century, with peak output occurring during a period of continuous mining from the 16th until the early 20th centuries (Hunter, 1885; Wilson and Flett, 1921). The New Glencrieff Mine was the final mine in operation and closed in the late 1950s (Gillanders, 1981).

At its peak, the LWO was Scotland's primary Pb-Zn producer, with up to 400 kilotons (kt) of Pb and approximately 1 million oz of Ag extracted from galena, 10 kt of Zn from sphalerite, and minor Cu from chalcopyrite (Temple, 1954). Around 70 veins are recorded across the LWO. These veins extend laterally for up to 3 km, predominantly trend NW-SE, dip at angles greater than 60°, and vary in width from a few millimetres to over a metre.

The veins are confined to the northwest of the district by the NE-SW trending Leadhills Fault and its associated imbricate zone of cherts, mudstone, and pillow basalts of the Crawford Group and Moffat Shale Group (Temple, 1954; Wilson and Flett, 1921; Mackay, 1959). Ore mineralisation is hosted in fault-controlled fracture-related veins, breccia fracture-fill, bands, and infilled open spaces within the Portpatrick Formation and Moffat Shale Group (Brown, 1925; Hunter, 1885; Temple, 1954; Wilson and Flett, 1921).

The primary ore minerals include galena, sphalerite, and chalcopyrite, accompanied by common gangue minerals such as quartz, calcite, barite, and pyrite. Fe-bearing dolomite, historically termed "ankerite," is also present across the LWO. Small specimens of jamesonite ($Pb_4FeSb_6S_{14}$), a sulfosalt mineral, have been found associated with galena mineralisation (Borthwick, 1992)

Most mining operations across the LWO were shallow, with the deepest reaching approximately 530 m below the surface. Zoning of ore mineralisation was observed,

progressing from near-surface barite to galena in the upper levels (200 to 365 m below surface), and sphalerite typically occurring below the 365 m level (Wilson and Flett, 1921).

Alluvial gold, still panned today from nearby streams, is believed to have four potential sources: Lower Palaeozoic sedimentary rock, igneous origin (possibly Palaeogene basaltic dykes), glacial drift, and Permian red-bed and basaltic volcanics along Lower Palaeozoic structures (Leake et al., 1998).

Historic geochemical data

Sphalerite is recorded in most veins on the western side of the Leadhills and Wanlockhead Orefield (LWO) and becomes increasingly scarce toward the east (Temple, 1954). Quantitative spectrochemical analysis of Fe in sphalerite revealed an almost uniform Fe content of approximately 4.91 wt.% (Temple, 1954). Qualitative spectrochemical analysis further indicated that Cd and Co are uniformly present, with additional trace elements incorporated into the sphalerite including Cu, Ag, Ga, Ge, Ti, Sn, Pb, Tl, V (Temple, 1954). However, Temple (1954) did not provide methodological details for the spectrochemical analysis and no modern, replicable data of this kind is known.

Using an FeS-ZnS thermometer calculation from Kullerud (1953), Temple (1954) estimated a sphalerite precipitation temperature of approximately 190 °C. Silver was historically extracted from galena across the LWO at concentrations ranging from 7 to 11 ounces per ton, equivalent to roughly 200 to 300 ppm (Brown, 1925).

Antimony, Ti, V, Sn, and Bi are considered to be ubiquitous in LWO galena (Temple, 1954). Chalcopyrite is present in most veins but was only actively mined from two locations: Long Cleuch and the Katystaklin Vein (Wilson and Flett, 1921). Historical qualitative spectrochemical analysis of chalcopyrite revealed trace amounts of Ag, Pb, Mn, Co, and Ni (Temple, 1954).

In pyrite, enrichment of Ni and Co was documented in earlier Caledonian and greywacke-hosted pyrites, rather than in those associated with sulfide ore samples (Temple, 1954). Arsenides and secondary arsenates were recorded in low quantities from several mines. Notably, niccolite (NiAs) and cobaltite (CoAsS) were documented on the West Branch of the New Glencrieff Vein (Brown, 1925).

Secondary arsenate minerals were thought to be generally more common across the LWO (Brown, 1925), although no arsenic (As) was detected in galena, sphalerite, chalcopyrite, pyrite, calcite, aragonite, barytes, or witherite by Temple (1954).

Modern geochemical data and ore genesis models

Stable isotope (H, O) analysis of fluid inclusions associated with ore-phase mineralisation indicates that the mineralising fluids were low temperature (<150 °C), high salinity (~19 to 30 equiv. wt.% NaCl + $CaCl_2$) modified meteoric waters (Samson and Banks, 1988). These findings link heat flow and heat sources to crustal fluid convection, with no magmatic influence, during a period of extensional tectonics in the Lower Carboniferous (Dinantian) (Samson and Banks, 1988).

Sulfur isotope analysis of sulfide and sulfate minerals by Pattrick and Russell (1989) and Anderson et al. (1989) supports the interpretation of deep-seated convection of hydrothermal fluids within the Lower Palaeozoic basement. This process likely scavenged sulfides from the basement, while sulfates were sourced from descending surface fluids. The convection system is estimated to have reached depths of up to 10 km (Samson and Banks, 1988; Anderson et al., 1989).

The tectonic context for the LWO remains speculative due to poor age constraints, which are based on K-Ar dating of fault gouge clays yielding an age range of 320–265 Ma (Ineson and Mitchell, 1974). Comparisons of ore fluids to meteoric sources have led to a Dinantian (359.2 to 326.4 Ma) age being proposed for ore mineralisation (Samson and Banks, 1988). Mixing of these fluids in the upper parts of the veins may have triggered ore precipitation and could have coincided with Carboniferous-age Irish Zn-Pb mineralisation (Anderson et al., 1989; Pattrick and Russell, 1989).

However, the timing of ore mineralisation at the LWO was recently revised using hematite (U/Th)/Ne geochronology. Dating of hematite that post-dates early Caledonian quartz veining and pre-dates the main phase of sulfide mineralisation revealed three hematite precipitation phases at approximately 230 Ma, 200 Ma, and 155 Ma. These results suggest that sulfide ore mineralisation is more likely to be Triassic/Jurassic in age, rather than Carboniferous as previously proposed (Currie, 2024).

Further insights into ore-forming processes were gained through helium (He) and sulfur (S) isotope data, which indicate that sulfur and metals were sourced from the underlying

basement. The He isotope composition of ore sulfides is crustal, with the highest recorded $^{3}He/^{4}He$ ratio being less than 1% of the typical mantle signature; implying that mantle-derived heat from deep magmatic bodies was not the heat source for LWO ore fluids (Currie, 2024).

In contrast, helium isotope analysis has demonstrated that Irish-type Pb-Zn mineralisation is unequivocally linked to a mantle-derived heat source (Davidheiser-Kroll et al., 2014). The revised timing and heat source for the LWO strongly suggest that it does not represent an Irish-type Zn-Pb mineralisation style, despite similar geological settings and geographic proximity and linkages being made in previous studies (Anderson et al., 1989; Pattrick and Russell, 1989). Therefore, caution is advised when comparing these two Pb-Zn-rich systems in future UK mineral systems approaches to critical minerals exploration. Currie (2024) relates the main ore precipitation event at the LWO to a later, more widespread series of western European tectonic events associated with the breakup of Pangaea during the late Triassic to Jurassic periods, rather than the Carboniferous Irish-type Zn-Pb mineralisation.

Comparative ore fluid geochemistry in Uk Zn-rich deposits

Given that temperature and salinity of ore fluids is the primary controlling factor for Ga, Ge, and In incorporation into sphalerite and other sulfides, it is worth noting the geochemical similarities to other historic UK Pb-Zn deposits for future research purposes. The ore fluid geochemistry of the North Pennine orefield, documented by Sawkins (1966) and Bouch et al (2006 and 2008), records a low temperature (up to 220 °C but commonly < 150 °C) high salinity (up to 25 equiv. wt.% NaCl + $CaCl_2$) ore fluid (Cann and Banks, 2001; More et al., 1991; Moore, 1988). Similar ore fluid geochemistry is noted in the South Pennine orefield, with low temperatures (80 - 200 °C) and high salinities (18 – 24 equiv. wt.% NaCl) recorded (Rogers, 1977; Atkinson, 1983; Moore, 1980; and Hollis, 1998). Fluid inclusion data across the West Shropshire orefield shows mineralising fluid to be low temperature (100 – 180 °C) and highly saline (16-30 equiv. wt.% NaCl) (Pattrick and Bowell, 1991). The Llanrwst Orefield, North Wales, shows mineralising fluid to be low temperature (125 – 190 °C) high salinity (up to 26 equiv. wt.% NaCl) (Haggerty and Bottrell, 1997). Fluid inclusions from the polymetallic sulfide lodes of the SW of England indicate formation temperatures of between 300 and 220 °C and salinities below 8 wt% NaCl eq. (Alderton and Harmon, 1991). The epithermal veins of SW England, termed ‘crosscourse’, formed at low temperatures e (100–170 °C) and high salinity (19–27 equiv. wt% NaCl) (Scrivener et al., 1994; Gleeson et al., 2001).

Environmental impact of historic mining

Although measures under the Environmental Protection Act 1990 aimed at remediating mining-polluted areas are in place, mining-related pollution remains a persistent issue in the villages of Leadhills and Wanlockhead (Chandler, 2012). Levels of Fe, Pb, Zn, As, Cd, and Cu in mine run-off and stream water, as well as Pb, Fe, Mg, Cu, Zn, and Mn in spoil heaps, exceed UK Environmental Quality Standards (EQS) (Byrne and Yendell, 2020) and fail to meet the Water Framework Directive's requirements (Chukwura and Hursthouse, 2020).

Environmental factors, potentially toxic element concentrations in analysed water, and trace element concentrations in aqua regia extracts of mine spoil materials have been documented across multiple studies (Chukwura and Hursthouse, 2020). For example, trace element concentrations (mg/kg) from two sample locations include: Pb – 10.75, Fe – 5.05, Mg – 0.6, Cu – 0.21, Zn – 0.04, and Mn – 0.01. The Glengonnar Water is particularly affected, showing high levels of metal pollution (Rowan et al., 1995).

A survey of residents revealed elevated blood lead levels at 45–70% higher than those recorded in Moniaive, a geologically and societally similar village without historical Pb-Zn mining (Moffat, 1989). Likely exposure routes include contaminated water, dust, soil, and homegrown vegetables. The Scottish Environmental Protection Agency (SEPA) warns that any major disturbance of the waste could further degrade water quality.

Due to the buffering capacity of carbonate minerals present within the host rocks, waters in the area maintain an almost neutral pH (Chukwura and Hursthouse, 2020). Circum-neutral pH mine waters are commonly observed across UK metal mining sites, typically resulting from carbonate weathering or a lack of pyrite in the ore (Marquinez et al., 2021; Warrander and Pearce, 2007). Although carbonate weathering helps prevent acid mine drainage, high concentrations of dissolved metals in neutral mine drainage remain a significant environmental concern across as many as 260 abandoned UK mine sites (Jarvis et al., 2023 and references therein).

Samples and Methodology

Ten polished blocks hosted in resin were sourced from the National Museum of Scotland (NMS) Collection Centre, Edinburgh, Scotland, in autumn of 2024. Of the ten blocks obtained, the following five were analysed by LA-ICP-MS: 2013.3.1, 2013.3.4, and 2013.3.8 – Belton Grain; 2013.1.2 – Laverock Hall; 2013.3.3 – Bury Vein (labelled as Bury Vein, but may be Bay Vein; Pers. Comm. NMS); 2013.3.5 – New Glencrieff; 2013.3.7 – Straitstep; 2013.3.9 – Glengonnar Shaft; and 2013.3.10 and 2013.3.11 – Old Glencrieff (Fig. 2).

The polished blocks contained a mixture of sphalerite, galena, chalcopyrite, pyrite, and gangue minerals including quartz, calcite, dolomite (Fe, Mg, Mn species), and siderite (Fig. 3). All microscopy and LA-ICP-MS analyses were conducted at the British Geological Survey (BGS) site in Keyworth.

Microscopy was performed on carbon sputter-coated (≈25 nm) polished blocks using a Zeiss Sigma 300 variable pressure (VP) field emission gun (FEG) scanning electron microscope (SEM), fitted with twin Bruker Xflash 6|30, 30 mm, 129 eV energy dispersive X-ray (EDX) detectors running Bruker's Esprit software (version 2.5). SEM-EDX mapping was conducted at 15 kV accelerating voltage, 3 nA beam current, and a working distance of 10 mm. Qualitative compositional analyses of mineral phases were performed using this SEM-EDX system.

Element concentration data was collected by LA-ICP-MS at the Inorganic Geochemistry Facility at BGS, Keyworth. The analytical system consisted of an ESI/New Wave Research imageGEO19 (193 nm) laser coupled to an Agilent 8900 triple quadrupole ICP-MS. Analytical conditions included a 20 µm spot size, 40 Hz repetition rate, and fluence of 3.5 J/cm². Internationally recognised standards were used to bracket samples: NIST glass standards SRM610 and SRM612 (Jochum et al., 2005), and USGS GSD-1G and BCR-2G, which were analysed before and after each sample (Siu et al., 2023). Data reduction was conducted using Iolite v4 (Paton et al., 2011), employing the 3D trace elements data reduction system (Paul et al., 2023), a software package specifically designed for LA-ICP-MS data processing. Analytical uncertainties are quoted at the 2-sigma level (Horstwood et al., 2016).

Data processing followed the recommendations of Frenzel (2023), including log-transformation of initial concentration data, treatment of missing or below-detection-limit

values by assigning a positive low value, and awareness of biases from unbalanced data distribution. The geometric mean (GM) of element concentration data was used to avoid overestimation from outliers, and detection limit values were applied where appropriate.

Sampling bias may exist in this study, as most samples analysed were from the Wanlockhead portion of the orefield. This bias was beyond the control of the author, and access to underground mine sites is no longer possible.

Results

The following element concentrations were obtained by LA-ICP-MS for galena, chalcopyrite, sphalerite, and pyrite: Mg, Al, Si, Ca, Mn, Fe, Co, Ni, Cu, Zn, Ga, Ge, As, Mo, Ag, Cd, In, Sn, Sb, Te, Bi, Se, and Pb. A total of 202 individual points were analysed on galena (n=54), chalcopyrite (n=74), sphalerite (n=34), and pyrite (n=40). The full analytical dataset is available in Supplementary Data 1.

The following breakdown includes the GM and maximum concentration data in parts per million (ppm) for a selected suite of elements for each primary sulfide (Table 1). For galena, the GM for Ag and Sb are 16 and 75, respectively. For chalcopyrite, the GM of In, Sn, and Se concentrations are 21, 21 and 17, respectively. For sphalerite, the GM for Ge, Ag, and Cd concentrations are 200, 120 and 2400, respectively. And for pyrite, the GM of As is 25. For galena, maximum Ag and Sb are 520 and 1260, respectively. For chalcopyrite, maximum In, Sn, and Se concentrations are 150, 1950 and 260, respectively. For sphalerite, maximum Ge, Ag, and Cd concentrations are 860, 1670 and 5900, respectively. And for pyrite, the maximum As concentration is 12000.

Discussion

Trace element host phases and comparison to global ore deposits

Gallium, Ge, and In have been identified as critical minerals, that is they are metals identified to have the greatest economic importance and the highest risk of supply disruption, with the potential to occur across the LWO (Deady et al., 2023). Based on the LA-ICP-MS concentration data presented in Table 1, the most likely host for Ga and Ge is sphalerite and chalcopyrite for In. The most likely host phases for other elements of interest are sphalerite for Ag and Cd, galena for Sb, chalcopyrite for Se, and pyrite for As. The maximum

concentrations and geometric mean values of Ga, Ge, and In as well as Sb, Se and Ag to crustal abundance and typical ore mineralisation concentrations are presented in Table 2.

Gallium concentration in the upper continental crust is recommended to be 17.5 ppm (Rudnick and Gao, 2014). The primary global source of Ga is downstream treatment of residues from aluminium processing with around 5–10% from sphalerite (Zn) processing (Nassar et al., 2015; Graedel et al., 2022; Idoine et al., 2024). In bauxite, Ga concentration is typically around 50 ppm. In the LWO, Ga in sphalerite has maximum and GM values of 140 and 6 ppm, respectively. Therefore, the maximum value of Ga in sphalerite at LWO is slightly elevated compared to general crustal abundance and bauxite ores. However, in sulfide ores where Ga is processed as a by-product of Zn processing, Ga values can reach >1000 ppm and averages are into the 100s of ppm (Foley et al., 2017). Sulfide mineralisation at LWO is therefore unlikely to be economically prospective for Ga, but further study of Ga deportment in sphalerite at LWO may provide insight into ore forming processes across the orefield.

Germanium concentration in the upper continental crust is recommended to be 1.4 ppm (Rudnick and Gao, 2014). Germanium is found in a range of sulfide minerals from a plethora of deposit types, but worldwide production is mostly from low temperature stratiform and strata-bound sphalerite deposits (Shanks III et al., 2017). It is estimated that the majority of worldwide production of Ge is sourced from the processing of Zn ore and the rest from coal fly ash and recycled metals on a 60/40 ratio (Moskalyk, 2004; Mudd et al., 2024; Idoine et al., 2024; Graedel et al., 2022; Nassar et al., 2015). Where Ge is processed during Zn ore refining, such as at the Red Dog SHMS deposit in Alaska, concentrations range from around 100 to 250 ppm (Kelly et al., 2004). At the Noailhac-Saint Salvy deposit, a polymetallic vein-type deposit near Tarn, France, around 400 t of Ge was historically produced from around 550 kt of Zn ore, grading at around 750 ppm Ge (Belissont et al., 2014). In Irish Zn-Pb deposits, Ge is known to reach around 900 ppm in sphalerite, 1000 ppm in tennantite, and 1300 ppm in galena though Ge has never been processed from this deposit type (Wilkinson et al., 2005). A recent study on the Lisheen Zn-Pb deposit, the second largest of the Irish Orefield, reveals Ge concentration in sphalerite to be between 10s and 100s of ppm which is deemed to be commercially viable (Frenzel et al., 2025). For coal and fly ash, the Lincang Mine, China is known to have around 1 kt of Ge at a grade of around 850 ppm (Hu et al., 2009). In the LWO, Ge in sphalerite has maximum and GM values of 860 and 200 ppm, respectively. Thus, the GM of Ge in sphalerite at the LWO is comparable to that at Red Dog, Alaska with maximum values comparable to that of St Salvy and Lincang. Further work is recommended to better understand the geographic distribution of sphalerite-bearing veins and associated spoil heaps and tailings at LWO and to assess their Ge potential.

Indium concentration in the upper continental crust is recommended to be 0.056 ppm (Rudnick and Gao, 2014). Indium is a by-product of Zn production primarily from Zn-sulfide deposits (90%) but can also be produced from Sn and Cu deposits (10%) (Lokanc et al., 2015; Werner et al., 2017). Around half of by-product In production comes from VMS and SHMS deposits in China with the remaining amount from MVT, though it is not fully known which deposits feed into the Zn smelting feedstock in China (Shanks III et al., 2017). Average In concentrations of around 200 ppm and 300 ppm are reported in sphalerite at the Loachang VMS and Daboshan SEDEX deposits, China (Ye et al., 2011). In polymetallic vein-type deposits like the Mount Pleasant In-bearing tin deposit, Canada, with In resources of around 620 t, sphalerite is reported to contain up to 6.90 wt % (69,000 ppm) In (Sinclair et al., 2006). Across southwest England, In concentration in skarn and 'crosscourse' related chalcopyrite, sphalerite, and stannite group minerals reaches a maximum of 2200 ppm, 14200 ppm, and 6800 ppm (Andersen et al., 2016). Thus, the GM and maximum In concentrations in chalcopyrite at the LWO are not comparable to economically exploited deposits. However, like Ga, further study of In deportment in chalcopyrite at LWO may provide insight into ore forming processes across the orefield.

Antimony concentration in the upper continental crust is recommended to be 0.4 ppm (Rudnick and Gao, 2014). Most of the global Sb production comes from the mining of primary carbonate replacement Sb deposits (60%) as well as stibnite-bearing vein-type deposits (~28%) and reduced magmatic and hot spring deposits (~12%) (Schwarz-Schampera, 2014). These deposits can form in many geological settings including peripheral zones of orogenic Au and porphyry Cu and Mo deposits, polymetallic vein deposits, or as stand-alone vein-type deposits (Seal II et al., 2017). These deposit styles tend to contain tens of wt % Sb in stibnite. Alternative sources of Sb, like from the refining of galena, can produce 99.99% pure Sb (Zhou et al., 2023). In their study, Zhou et al. (2023) state the need for alternative sources of high purity Sb to alleviate pressures on the Sb mining sector and create a more stable, secure, and environmentally conscious supply of Sb. In the LWO, Sb in galena has maximum and GM values of 1260 and 75 ppm, respectively. In conjunction with known Sb-bearing mineral deposits in the UK (Deady et al., 2019; Knight et al., 2016; Macgregor et al., 2015; Deady et al., 2023), further study on Sb extraction methods from galena could lead to a better understanding of unconventional Sb processing potential for the UK.

Silver concentration in the upper continental crust is recommended to be 53 ppm (Rudnick and Gao, 2014). Most of the global Ag production is as a by-product of Pb-Zn mining, closely

followed by Ag production from Cu and Au deposits (Idoine et al., 2024). Silver deposits are found in a variety of geological settings such as VMS, SHMS, lithogene and magmatic-hydrothermal. Average Ag grades across these deposit types can range from around 33 ppm (VMS) to more than 600 ppm in higher grade veins related to magmatic-hydrothermal deposits (Graybeal and Vikre, 2010). Historically in the UK, Ag was recovered from galena in many ore deposits. In the North Pennine orefield, where around 5.45 million oz (170 tonnes) of Ag was recovered from over 1.5 million tonnes of Pb concentrates, Ag concentration average of roughly 100 – 250 ppm in galena (Dunham, 1990). Total Ag production from galena for northeast Wales is thought to be around 2.5 million oz (~76 tonnes) (Burt and Waite, 1992). In the southwest of England, Ag was predominantly sources from galena, but native silver, and other sulfides, oxides, chlorides, and Cu-ore containing Ag are known (Dines, 1956). Silver-bearing ore were typically found in 'crosscourses', epigenetic vein mineralisation and were associated with Bi, Co, Ni, and Sb (Dines, 1956). It is thought that around 2000 tonnes of Ag was raised in the 19th century across southwest England (Dines, 1956). At the LWO, Ag in galena has maximum and GM values of 520 and 16 ppm, respectively, and in sphalerite a maximum concentration of 1700 ppm and a GM of 120 ppm. Therefore, Ag concentrations at the LWO are comparable or even greater than typical values of Ag-rich ore deposits. Further work is recommended to better understand the geographic distribution of LWO Ag-bearing veins and associated spoil heaps and tailings.

Selenium concentration in the upper continental crust is recommended to be 0.09 ppm (Rudnick and Gao, 2014). Around 80% of global production of Se is obtained as a by-product of Cu refining, specifically from anode slimes generated in electrolytic production of Cu (Schulz, 2017). Minor amounts of Se have been produced from Ni, Pb and Zn refining (Schulz, 2017). Per metric ton of recoverable electrolytic Cu, typical recovery values of Se range between 215 g to 640 g/ton (Butterman and Brown Jr., 2004; George and Wagner, 2009). At the LWO, maximum and GM values for Se in chalcopyrite are 260 and 17 ppm, respectively. Although these values are not viably economic for recovery since the LWO is not well endowed with chalcopyrite mineralisation, Se values are noted since Se can cause human health issues. Chronic exposure to subacute levels of Se can lead to brittle hair and nails, skin lesions, and neurological disturbances (Winkel et al., 2012).

Sphalerite trace element comparison to global dataset

Considering the previous comparison to crustal abundances and typical ore grades for each element of interest, the Ge concentration in LWO sphalerite is of the greatest interest. Further comparison to ore deposits that have had sphalerite trace element geochemistry

assessed using LA-ICP-MS confirms that sphalerite from LWO may be anomalously enriched in Ge (Fig. 4; Table 3). It should be noted that our study lacks a deposit-wide assessment of vein, spoil heap, and tailings analysis and has only 34 LA-ICP-MS point analyses carried out on a single sample. However, the initial analyses are promising and merits further orefield-wide assessment, perhaps in conjunction with other Zn-rich areas like West Shropshire, northeast Wales, and the North and South Pennine orefields based on similar ore fluid geochemistry in these regions.

Cadmium and Arsenic

The GM and maximum values for concentrations of deleterious elements are 2400 and 5900 ppm for Cd in sphalerite, respectively, and 25 and 12000 for As in pyrite, respectively. It is known that Cd and As levels in mine run-off and stream waters within and downstream of the LWO exceed UK Environmental Quality Standards (EQS) (Byrne and Yendell, 2020) and fail to meet the Water Framework Directive's requirements (Chukwura and Hursthouse, 2020), and it is now confirmed that these elements are primarily hosted in sphalerite and pyrite.

Seven sources of dissolved Zn and Cd in waters have been identified including Bay Mine Adit (18%), Meadowfoot Adit and Glenglass Level No. 2 (18%), Glenglass Level (16%), and the Wanlock Water upstream of Bay Mine Adit (9%) (Byrne and Yendell, 2020). The significance of the latter is that the Wanlock Water upstream of Bay Mine Adit was mostly dry during sampling. Therefore, the sampled water was probably ground or surface water from the hyporheic zone further upstream which had infiltrated mined strata or made ground in the floodplain and re-emerged at the sampling point (Byrne and Yendell, 2020).

Total recoverable and filtered (0.45 μm filter) dissolved loads of Cd are found in the same locations as Zn across the study area of Byrne and Yendell (2020), which is consistent with our finding that Cd is hosted in sphalerite. Interestingly, Byrne and Yendell (2020) found that total and dissolved Pb in waters was primarily sourced from Queensbury Tailings Ponds and wetland area mine waste deposits, whereas Zn and Cd were mainly sourced from mine waters emerging into the Wanlock Water via Bay Mine Adit, Glenglass Level, Meadowfoot Adit, and Glenglass Level No. 2. Notable Zn and Cd contributions occur from the Queensbury Tailings Pond, too.

No data exists on the source(s) of As, but data from this study suggests pyrite is likely to be the main source of As and attention should be paid to any veins, spoil heaps, and tailings ponds with elevated pyrite mineralisation.

Conclusion

The LA-ICP-MS concentration data from the LWO reveals that the critical minerals Ga and Ge are primarily hosted in sphalerite, while In is found in chalcopyrite. Other notable elements like Ag and Cd are also in sphalerite, while Sb is hosted in galena, Se in chalcopyrite, and As in pyrite. The concentration of these elements varies, but Ge stands out as being particularly enriched. Germanium in sphalerite at the LWO may therefore merit further study since concentrations and the GM are comparable to significant global Ge resources like Red Dog in Alaska.

Gallium concentrations in sphalerite and In concentrations in chalcopyrite are slightly elevated compared to crustal abundances, but not at levels comparable to exploited resources. Antimony in galena and Ag in both sphalerite and galena are notable, with Ag concentrations in sphalerite comparable to, or greater than typical values in some Ag-rich ore deposits. Further study on how to best extract Ag from sphalerite and Sb from galena would be beneficial in a UK mineral deposit context. The study therefore recommends further investigation into the geographic distribution of sphalerite-bearing veins and associated spoil heaps and tailings at LWO to assess the potential for Ge extraction, as well as other notable elements.

This study found high concentrations of Cd and As in sphalerite and pyrite, respectively. Cd and As levels in waters within and downstream of the LWO exceed UK Environmental Quality Standards and fail to meet the Water Framework Directive's requirements. From previous work, dissolved Zn and Cd in water were identified near Bay Mine adit, Meadowfoot Adit, Glenglass Level No.2, Glenglass Level, and Wanlock Water upstream of Bay Mine Adit. The latter was mostly dry during sampling, indicating the sampled water was likely from the hyporheic zone further upstream. Total and dissolved loads of Cd were found in the same locations as Zn, consistent with Cd being hosted in sphalerite in data from our study. Pb in waters was primarily sourced from Queensbury Tailings Ponds and wetland area mine waste deposits, but Zn was predominantly found in water from mine adit outflow and in the Queensbury Tailings Ponds. Pyrite is likely the main source of As based on our study.

Future work

A more geographically inclusive survey of the vein mineralisation and adjacent spoil heap and tailings ponds' mineralogy should be undertaken to identify potentially prospective and/or hazardous areas across the LWO. In doing so, an attempt to quantify remaining resources across the LWO could be of interest.

Elevated Se concentrations in chalcopyrite are unlikely to be economically viable due to lack of Cu mineralisation across the entire LWO, but acute overexposure to Se does pose health risks, such as brittle hair and nails, skin lesions, and neurological disturbances, therefore having a better understanding of Cu mineralisation across the entire orefield would be beneficial for health purposes.

Further study on the effects of climate change and the breakdown and dispersion of hazardous materials from ore mineralisation, mine waste, and tailings ponds should be undertaken to help mitigate and prepare for any ill effects. For example, understanding the effects of increasing precipitation and temperature on the breakdown of ore phases and the subsequent release of Cd, As, and other environmental deleterious elements into water courses would be of particular interest.

Finally, further study on substitution mechanisms for Ge in sphalerite may also help with any future mineral processing research at LWO, this could be done using atom probe tomography, for example.

References

Alderton, D.H.M. and Harmon, R.S. 1991. Fluid inclusion and stable isotope evidence for the origin of mineralizing fluids in south-west England. Mineralogical Magazine, 55(381), pp.605-611.Andersen, J.C., Stickland, R.J., Rollinson, G.K. and Shail, R.K. 2016. Indium mineralisation in SW England: host parageneses and mineralogical relations. Ore Geology Reviews, 78, pp.213-238.

Anderson, I., Andrew, C., Ashton, J., Boyce, A., Caulfield, J., Fallick, A. & Russell, M. 1989. Preliminary sulphur isotope data of diagenetic and vein sulphides in the Lower Palaeozoic strata of Ireland and southern Scotland: implications for Zn+ Pb+ Ba mineralization. Journal of the Geological Society, 146, 715–720.

Atkinson, P. 1983. A fluid inclusion and geochemical investigation of the fluorite deposits of the southern Pennine orefield (Doctoral dissertation, University of Leicester). Available at https://figshare.le.ac.uk/articles/thesis/A_Fluid_Inclusion_and_Geochemical_Investigation_of_the_Fluorite_Deposits_of_the_Southern_Pennine_Orefield/10101302?file=18208832

Barnes, S.J., Cruden, A.R., Arndt, N. & Saumur, B.M. 2016. The mineral system approach applied to magmatic Ni–Cu–PGE sulphide deposits. Ore Geology Reviews, 76, 296–316.

Belissont, R., Boiron, M.C., Luais, B. & Cathelineau, M. 2014. LA-ICP-MS analyses of minor and trace elements and bulk Ge isotopes in zoned Ge-rich sphalerites from the Noailhac–Saint-Salvy deposit (France): insights into incorporation mechanisms and ore deposition processes. Geochimica et Cosmochimica Acta, 126, 518–540.

Borthwick, C.W. 1992. 'Scottish Borders geology: an excursion guide', in McAdam, A.D., Clarkson, E.N.K. and Stone, P. (eds.) Scottish Borders geology: an excursion guide. Edinburgh: Scottish Academic Press (for Edinburgh Geological Society).

Bouch, J.E., Naden, J., Shepherd, T.J., McKervey, J.A., Young, B., Benham, A.J. and Sloane, H.J., 2006. Direct evidence of fluid mixing in the formation of stratabound Pb–Zn–Ba–F mineralisation in the Alston Block, North Pennine Orefield (England). Mineralium Deposita, 41(8), pp.821-835.

Bouch, J., Naden, J., Shepherd, T., Young, B., Benham, A., McKervey, J. and Sloane, H. 2008. Stratabound Pb-Zn-Ba-F mineralisation in the Alston Block of the North Pennine Orefield (England): origins and emplacement. Nottingham: British Geological Survey. British Geological Survey Report RR/08/006.

Burt, R. and Waite, P. 1992. The Mines of Flintshire & Denbighshire: Metalliferous and Associated Minerals 1845–1913. Vol. 10. Liverpool: Liverpool University Press.

Cailteux, J., Kampunzu, A., Lerouge, C., Kaputo, A. & Milesi, J. 2005. Genesis of sediment-hosted stratiform copper–cobalt deposits, central African Copperbelt. Journal of African Earth Sciences, 42, 134–158.

Cann, J.R., Banks, D.A. 2001. Constraints on the genesis of the mineralization of the Alston Block, Northern Pennine Orefield, northern England. Proceedings of the Yorkshire Geological Society. 53 (3), 187-195

Chukwura, U.O. & Hursthouse, A.S. 2020. Evaluating controls on potentially toxic element release in circum-neutral mine water: a case study from the abandoned Pb–Zn mines of Leadhills and Wanlockhead, South of Scotland, United Kingdom. Environmental Earth Sciences, 79, 363.

Cook, N.J., Ciobanu, C.L., Meria, D., Silcock, D. & Wade, B. 2013. Arsenopyrite–pyrite association in an orogenic gold ore: tracing mineralization history from textures and trace elements. Economic Geology, 108, 1273–1283.

Cook, N.J., Ciobanu, C.L., Pring, A., Skinner, W., Shimizu, M., Danyushevsky, L., Saini-Eidukat, B. & Melcher, F. 2009. Trace and minor elements in sphalerite: a LA-ICPMS study. Geochimica et Cosmochimica Acta, 73, 4761–4791.

Davidheiser-Kroll, B., Stuart, F. & Boyce, A. 2014. Mantle heat drives hydrothermal fluids responsible for carbonate-hosted base metal deposits: evidence from $^{3}He/^{4}He$ of ore fluids in the Irish Pb–Zn ore district. Mineralium Deposita, 49, 547–553.

Deady, E., Moore, K., Goodenough, K., Rollinson, G., Boyce, A., Sośnicka, M. & Shail, R. 2019. Controls on antimony mineralisation in 'cross-course' veining in SW England. Applied Earth Science, 128, 44–44.

Dines, H.G., 1956. The metalliferous mining region of south-west England (Vol. 1). HM Stationery Office.

Dunham, K C. 1990. Geology of the Northern Pennine Orefield, Volume 1 Tyne to Stainmore (2nd edition). Economic Memoir of the British Geological Survey, sheets 19 and 25 and parts of 13, 24, 26, 31, 32 (England and Wales).

Fleischer, M. 1955. Minor elements in some sulfide minerals. Economic Geology, 50, 1024.

Frenzel, M. 2023. Making sense of mineral trace-element data – how to avoid common pitfalls in statistical analysis and interpretation. Ore Geology Reviews, 105566.

Frenzel, M., Hirsch, T. & Gutzmer, J. 2016. Gallium, germanium, indium, and other trace and minor elements in sphalerite as a function of deposit type – a meta-analysis. Ore Geology Reviews, 76, 52–78.

Frenzel, M., Röhner, M., Cook, N.J., Gilbert, S., Ciobanu, C.L. and Güven, J.F. 2025. Mineralogy, mineral chemistry, and genesis of Cu-Ni-As-rich ores at Lisheen, Ireland. Mineralium Deposita, 60(1), pp.113-143.

Gemmell, C.A., Neill, I., Wildman, M., MacRae, C., Currie, D. & Einsle, J.F. 2025. New integrations of U–Pb zircon data from Caledonian intrusions in the Southern Uplands of Scotland. Lithos, 494, 107941.

George, L., Cook, N.J. & Wade, B.P. 2015. Trace and minor elements in galena: a reconnaissance LA-ICP-MS study. American Mineralogist, 100, 548–569.

George, L.L., Cook, N.J. & Ciobanu, C.L. 2016. Partitioning of trace elements in co-crystallized sphalerite–galena–chalcopyrite hydrothermal ores. Ore Geology Reviews, 77, 97–116.

Gillanders, R. 1981. The Leadhills–Wanlockhead district, Scotland. Mineralogical Record, 12, 235–250.

Gleeson, S.A., Wilkinson, J.J., Stuart, F.M. and Banks, D.A. 2001. The origin and evolution of base metal mineralising brines and hydrothermal fluids, South Cornwall, UK. Geochimica et Cosmochimica Acta, 65(13), pp.2067-2079.

Graedel, T., Reck, B.K. & Miatto, A. 2022. Alloy information helps prioritize material criticality lists. Nature Communications, 13, 150.

Graybeal, F. & Vikre, P.G. 2010. A review of silver-rich mineral deposits and their metallogeny. In: The Challenge of Finding New Mineral Resources: Global Metallogeny, Innovative Exploration, and New Discoveries. SEG Special Publication 15 Vol. 1, 85–117.

Groves, D.I., Santosh, M. & Zhang, L. 2020. A scale-integrated exploration model for orogenic gold deposits based on a mineral system approach. Geoscience Frontiers, 11, 719–738.

Haggerty, R. and Bottrell, S.H. 1997. The genesis of the Llanrwst and Llanfair veinfields, North Wales: evidence from fluid inclusions and stable isotopes. Geological Magazine, 134(2), pp.249-260.

Hamaguchi, H. & Kuroda, R. 1959. Silver content of igneous rocks. Geochimica et Cosmochimica Acta, 17, 44–52.

Hines, R., Paterson, S.R., Memeti, V. & Chambers, J.A. 2018. Nested incremental growth of zoned upper crustal plutons in the Southern Uplands Terrane, UK: fractionating, mixing, and contaminated magma fingers. Journal of Petrology, 59, 483–516.

Hollis, C. 1998. Reconstructing fluid history: an integrated approach to timing fluid expulsion and migration on the Carboniferous Derbyshire Platform, England. Geological Society, London, Special Publications, 144(1), pp.153-159.

Horstwood, M.S., Košler, J., Gehrels, G., Jackson, S.E., McLean, N.M., Paton, C., Pearson, N.J., Sircombe, K., Sylvester, P. & Vermeesch, P. 2016. Community-derived standards for LA-ICP-MS U-(Th-) Pb geochronology – uncertainty propagation, age interpretation and data reporting. Geostandards and Geoanalytical Research, 40, 311–332.

Hu, R.Z., Qi, H.W., Zhou, M.F., Su, W.C., Bi, X.W., Peng, J.T. & Zhong, H. 2009. Geological and geochemical constraints on the origin of the giant Lincang coal seam-hosted germanium deposit, Yunnan, SW China: a review. Ore Geology Reviews, 36, 221–234.

Hu, Z. & Gao, S. 2008. Upper crustal abundances of trace elements: a revision and update. Chemical Geology, 253, 205–221.

Hunter, J.R. 1885. The Silurian districts of Leadhills and Wanlockhead, their early and recent mining history. Transactions of the Geological Society of Glasgow, 7, 373–392.

Huston, D. & Bastrakov, E. 2024. Germanium, indium, gallium and cadmium in zinc ores: a mineral system approach. Australian Journal of Earth Sciences, 71, 1125–1155.

Ineson, P. & Mitchell, J. 1974. K–Ar isotopic age determinations from some Scottish mineral localities. Transactions of the Institution of Mining and Metallurgy, 83, B13–18.

International Energy Association. 2025. Global Critical Minerals Outlook 2025. IEA, Paris. Available: https://www.iea.org/reports/global-critical-minerals-outlook-2025 (Licence: CC BY 4.0).

Jarvis, A.P., Gandy, C.J. & Webb, J.A. 2023. Controls on the generation and geochemistry of neutral mine drainage: evidence from Force Crag Mine, Cumbria, UK. Minerals, 13, 592. Available: https://doi.org/10.3390/min13050592

Jochum, K.P., Nohl, U., Herwig, K., Lammel, E., Stoll, B. & Hofmann, A.W. 2005. GeoReM: a new geochemical database for reference materials and isotopic standards. Geostandards and Geoanalytical Research, 29, 333–338.

Kelley, K.D., Leach, D.L., Johnson, C.A., Clark, J.L., Fayek, M., Slack, J.L., Anderson, V.M., Ayuso, R.A. & Ridley, W.I. 2004. Textural, compositional, and sulfur isotope variations of sulfide minerals in the Red Dog Zn–Pb–Ag deposits, Brooks Range, Alaska:

implications for ore formation. Economic Geology, 99, 1509–1532. Available: https://doi.org/10.2113/gsecongeo.99.7.1509

Knight, H., Deady, É., Gunn, A., Moore, K. & Naden, J. 2016. Ore fluid characteristics of antimony deposits in South West England: new insights into ore genesis in Wadebridge–Port Isaac and Herodsfoot. Applied Earth Science, 125, 89–89.

Large, R.R., Danyushevsky, L., Hollit, C., Maslennikov, V., Meffre, S., Gilbert, S., Bull, S., Scott, R., Emsbo, P. & Thomas, H. 2009. Gold and trace element zonation in pyrite using a laser imaging technique: implications for the timing of gold in orogenic and Carlin-style sediment-hosted deposits. Economic Geology, 104, 635–668.

Leake, R., Chapman, R.J., Bland, D., Stone, P., Cameron, D. & Styles, M. 1998. The origin of alluvial gold in the Leadhills area of Scotland: evidence from interpretation of internal chemical characteristics. Journal of Geochemical Exploration, 63, 7–36.

Leggett, J., McKerrow, W.T. & Eales, M. 1979. The Southern Uplands of Scotland: a Lower Palaeozoic accretionary prism. Journal of the Geological Society, 136, 755–770.

Livingstone, A., Smith, C.G. & MacFadyen, C.C.J. 2022. Scottish mineral Geological Conservation Review sites – hydrothermal veins and mineral assemblages. Proceedings of the Geologists' Association, 133, 367–395. Available: https://doi.org/10.1016/j.pgeola.2020.09.002

Lottermoser, B.G. 2011. Recycling, reuse and rehabilitation of mine wastes. Elements, 7, 405–410.

Łuszczak, K., Persano, C. & Stuart, F. 2018. Early Cenozoic denudation of central west Britain in response to transient and permanent uplift above a mantle plume. Tectonics, 37, 914–934.

Macgregor, K., MacKinnon, G., Farmer, J.G. & Graham, M.C. 2015. Mobility of antimony, arsenic and lead at a former antimony mine, Glendinning, Scotland. Science of the Total Environment, 529, 213–222.

Mange, M.A., Dewey, J.F. & Floyd, J.D. 2005. The origin, evolution and provenance of the Northern Belt (Ordovician) of the Southern Uplands Terrane, Scotland: a heavy mineral perspective. Proceedings of the Geologists' Association, 116, 251–280. Available: https://doi.org/10.1016/S0016-7878(05)80045-8

Márquez-Zavalía, M.F., Vymazalová, A., Galliski, M.Á., Laufek, F., Tuhý, M., Watanabe, Y. and Bernhardt, H.J., 2024. Indium-copper-rich sphalerite from the Restauradora vein, Capillitas, Catamarca, Argentina. Resource Geology, 74(1), p.e12325.

Marquinez, Y., Bowell, R.J., Jones, T. & Braham, P. 2021. Geochemical sources and long-term implications of mine waste weathering, Cwmystwyth Mine, Wales. Available: https://www.imwa.info/docs/imwa_2021/IMWA2021_Marquinez_374.pdf

McCuaig, T.C., Beresford, S. & Hronsky, J. 2010. Translating the mineral systems approach into an effective exploration targeting system. Ore Geology Reviews, 38, 128–138.

McKerrow, W., Leggett, J. & Eales, M. 1977. Imbricate thrust model of the Southern Uplands of Scotland. Nature, 267, 237–239.

McMillan, A. & Brand, P. 1995. Depositional setting of Permian and Upper Carboniferous strata of the Thornhill Basin, Dumfriesshire. Scottish Journal of Geology, 31, 43–52.

Mighall, T., Martinez Cortizas, A., Silva Sanchez, N., Foster, I.D., Singh, S., Bateman, M. & Pickin, J. 2014. Identifying evidence for past mining and metallurgy from a record of metal contamination preserved in an ombrotrophic mire near Leadhills, SW Scotland, UK. The Holocene, 24, 1719–1730.

Miles, A., Graham, C., Hawkesworth, C., Gillespie, M., Dhuime, B. & Hinton, R. 2014. Using zircon isotope compositions to constrain crustal structure and pluton evolution: the Iapetus Suture Zone granites in northern Britain. Journal of Petrology, 55, 181–207.

Moats, M., Alagha, L. & Awuah-Offei, K. 2021. Towards resilient and sustainable supply of critical elements from the copper supply chain: a review. Journal of Cleaner Production, 307, 127207.

Moffat, W.E. 1989. Blood lead determinants of a population living in a former lead mining area in Southern Scotland. Environmental Geochemistry and Health, 11, 3–9.

More, A.P., Vaughan, D.J. and Ashworth, J.R., 1991. Banded sphalerite from the North Pennine orefield. Mineralogical Magazine, 55 (380), pp.409-416.

Moore, G.R., 1980 A chemical and isotopic study of fluid inclusions from the northern Pennine orefield. Doctoral dissertation. Durham University. Available at: Durham University eTheses (https://etheses.dur.ac.uk/1098/1/1098.pdf?EThOS%20(BL)) (Accessed: 5 September 2025).

Moskalyk, R.R. 2004. Review of germanium processing worldwide. Minerals Engineering, 17, 393–402.

Moyo, A., Parbhakar-Fox, A., Meffre, S. & Cooke, D.R. 2023. Geoenvironmental characterisation of legacy mine wastes from Tasmania – environmental risks and opportunities for remediation and value recovery. Journal of Hazardous Materials, 454, 131521.

Mudd, G., Josso, P., Shaw, R., Luce, A., Singh, N., Horn, S., Bide, T., Currie, D., Elliott, H. & Grant, H. 2024. UK 2024 criticality assessment.

Nassar, N.T., Graedel, T.E. & Harper, E.M. 2015. By-product metals are technologically essential but have problematic supply. Science Advances, 1, e1400180. Available: https://doi.org/10.1126/sciadv.1400180

Oliveira, M.L., Ward, C.R., Izquierdo, M., Sampaio, C.H., de Brum, I.A., Kautzmann, R.M., Sabedot, S., Querol, X. & Silva, L.F. 2012. Chemical composition and minerals in pyrite ash of an abandoned sulphuric acid production plant. Science of the Total Environment, 430, 34–47.

Paton, C., Hellstrom, J., Paul, B., Woodhead, J. & Hergt, J. 2011. Iolite: freeware for the visualisation and processing of mass spectrometric data. Journal of Analytical Atomic Spectrometry, 26, 2508–2518.

Pattrick, R.A.D. and Bowell, R.J. 1991. The genesis of the West Shropshire Orefield: evidence from fluid inclusions, sphalerite chemistry, and sulphur isotopic ratios. Geological Journal, 26(2), pp.101-115.

Pattrick, R. & Russell, M. 1989. Sulphur isotopic investigation of Lower Carboniferous vein deposits of the British Isles. Mineralium Deposita, 24, 148–153.

Paul, B., Petrus, J., Savard, D., Woodhead, J., Hergt, J., Greig, A., Paton, C. & Rayner, P. 2023. Time resolved trace element calibration strategies for LA-ICP-MS. Journal of Analytical Atomic Spectrometry. 38, 1995-2006.

Pickett, E. & Floyd, J. 2003. Geology of the Leadhills District: a brief explanation of the geological map sheet 15E Leadhills. British Geological Survey. ISBN: 0852724535.

Rowan, J.S., Barnes, S., Hetherington, S., Lambers, B. & Parsons, F. 1995. Geomorphology and pollution: the environmental impacts of lead mining, Leadhills, Scotland. Journal of Geochemical Exploration, 52, 57–65.

Samson, I. & Banks, D. 1988. Epithermal base-metal vein mineralization in the Southern Uplands of Scotland: nature and origin of the fluids. Mineralium Deposita, 23, 1–8.

Sawkins, F.J., 1966. Ore genesis in the North Pennine orefield, in the light of fluid inclusion studies. Economic Geology, 61(2), pp.385-401.

Schulz, K.J. 2017. Critical mineral resources of the United States: economic and environmental geology and prospects for future supply. US Geological Survey. ISBN: 1411339916.

Schwarz-Schampera, U. 2014. Antimony. In: Gunn, G. (ed.) Critical Metals Handbook, 70–98.

Scrivener, R.C., Darbyshire, D.P.F. and Shepherd, T.J. 1994. Timing and significance of crosscourse mineralization in SW England. Journal of the Geological Society, 151(4), pp.587-590.

Seal II, R.R., Schulz, K.J., DeYoung, J.J.H., Sutphin, D.M., Drew, L.J., Carlin Jr, J.F. & Berger, B.R. 2017. Antimony. USGS Professional Paper 1802C. Reston, VA: US Geological Survey. Available: https://pubs.usgs.gov/publication/pp1802C

Shanks III, W.C.P., Kimball, B.E., Tolcin, A.C. & Guberman, D.E. 2017. Germanium and indium. USGS Professional Paper 1802I. Reston, VA: US Geological Survey. Available: https://pubs.usgs.gov/publication/pp1802I

Sillitoe, R.H. 2010. Porphyry copper systems. Economic Geology, 105, 3–41.

Sinclair, W., Kooiman, G., Martin, D. & Kjarsgaard, I. 2006. Geology, geochemistry and mineralogy of indium resources at Mount Pleasant, New Brunswick, Canada. Ore Geology Reviews, 28, 123–145.

Siu, I., Cui, J., Henderson, J., Crowther, A., Boivin, N., Fergadiotou, E., Blair, A., Ali, A.K. & Chenery, S. 2023. Early Islamic glass (7th–10th centuries AD) in Unguja Ukuu, Zanzibar: a microcosm of a globalised industry in the early ‘Abbasid period. PLOS ONE, 18, e0284867.

Stone, P., McMillan, A.A., Floyd, J.D., Barnes, R.P. and Phillips, E.R. 2012. South of Scotland 4th ed. British Geological Survey.

Stone, P. 2014. The Southern Uplands Terrane in Scotland – a notional controversy revisited. Scottish Journal of Geology, 50, 97–123.

Tanner, J.T. & Ehmann, W.D. 1967. The abundance of antimony in meteorites, tektites and rocks by neutron activation analysis. Geochimica et Cosmochimica Acta, 31, 2007–2026. Available: https://doi.org/10.1016/0016-7037(67)90140-8

Taylor, S.R. & McLennan, S.M. 1995. The geochemical evolution of the continental crust. Reviews of Geophysics, 33, 241–265.

Temple, A.K. 1954. The paragenetical mineralogy of the Leadhills and Wanlockhead lead and zinc deposits. University of Leeds. Available: https://etheses.whiterose.ac.uk/id/eprint/12756/1/668124.pdf

Turekian, K.K. & Wedepohl, K.H. 1961. Distribution of the elements in some major units of the Earth's crust. Geological Society of America Bulletin, 72, 175–192.

Vitti, C. & Arnold, B.J. 2022. The reprocessing and revalorization of critical minerals in mine tailings. Mining, Metallurgy & Exploration, 39, 49–54.

Warrander, R. & Pearce, N.J.G. 2007. Remediation of circum-neutral, low-iron waters by permeable reactive media. Available: https://www.imwa.info/docs/imwa_2007/IMWA2007_Warrender.pdf

Werner, T., Mudd, G.M. & Jowitt, S.M. 2017. The world's by-product and critical metal resources part III: a global assessment of indium. Ore Geology Reviews, 86, 939–956.

Whitney, D.L. and Evans, B.W. 2010. Abbreviations for names of rock-forming minerals. American mineralogist, 95(1), pp.185-187.

Wilkinson, J.J., Eyre, S.L. & Boyce, A.J. 2005. Ore-forming processes in Irish-type carbonate-hosted Zn–Pb deposits: evidence from mineralogy, chemistry, and isotopic composition of sulfides at the Lisheen mine. Economic Geology, 100, 63–86.

Wilson, G. & Flett, J. 1921. The lead, zinc, copper and nickel ores of Scotland. Special Reports on the Mineral Resources of Great Britain. Mems. Geol. Surv. Scotland, HMSO, 17.

Winkel, L.H., Johnson, C.A., Lenz, M., Grundl, T., Leupin, O.X., Amini, M. & Charlet, L. 2012. Environmental selenium research: from microscopic processes to global understanding. ACS Publications. [Accessed].

Ye, L., Cook, N.J., Ciobanu, C.L., Yuping, L., Qian, Z., Tiegeng, L., Wei, G., Yulong, Y. & Danyushevskiy, L. 2011. Trace and minor elements in sphalerite from base metal deposits in South China: a LA-ICPMS study. Ore Geology Reviews, 39, 188–217.

Zhou, Z., Xie, H., Wang, Y., Xiong, H., Wang, S., Li, L., Xu, B. & Yang, B. 2023. High-purity antimony sulfide condensate produced from heterogeneous antimony sulfide ore by directed volatilization in a vacuum ambient. Minerals Engineering, 191

Acknowledgements:

The authors would like to thank Dr. Bob Gooday at the National Museum of Scotland for supplying sample material from the Leadhills and Wanlockhead collection, Craig Woodward for assistance with map illustrations, Dr. Jeremy Rushton and Dr. Marli de Jongh for assistance with petrography, and Dr. Elliott Hamilton for assistance with LA-ICP-MS. D. Currie, H. Grant, and L.Tuffield publish with the permission of the Director of the British Geological Survey.

Funding:

This work was supported by the British Geological Survey via NERC national capability.

Author Contribution:

DC: Conceptualization, formal analysis, investigation, methodology, writing – original draft, writing – review & editing (lead), data curation (equal), supervision (supporting); AB conceptualization (supporting), writing – original draft, writing – review & editing (supporting), formal analysis (supporting), data curation (supporting), investigation (supporting); NB:

conceptualization (supporting), writing – original draft, writing – review & editing (supporting), supervising (lead); HG: data curation (supporting), validation (supporting), investigation (supporting); LT: data curation (equal), formal analysis (supporting), writing – review & editing (supporting), validation (supporting).

Competing interest:

The authors declare that they have no known competing financial interests or personal relationships that could have appeared to influence the work reported in this paper.

Data Availability:

The datasets generated during and/or analysed during the current study are available in the [NAME] repository, [PERSISTENT WEB LINK TO DATASETS].

Figure and table captions

Figure 1: Geological map of the Southern Upland Terrane (a) and Leadhills and Wanlockhead orefield (b) with ore veins in magenta. Maps based on Stone et al. (2012). Black box in right hand image is area in Figure 2. Contains OS data © Crown copyright and database rights 2025. Contains NEXTMap Britain elevation data from Intermap Technologies.

Figure 2: Map showing locations of villages, roads, the historic narrow-gauge railway, veins, trials, level mouths, shafts, rivers (waters) and reservoirs. Named veins and Glengonnar Shaft correspond to the rough locations of the samples in this study. Map adapted from Wilson and Flett (1921). Contains OS data © Crown copyright and database rights 2025. Contains NEXTMap Britain elevation data from Intermap Technologies.

Figure 3: BSE images of each sample analysed by LA-ICP-MS. A) Sample 2013-3-1 highlighting cogenetic cpy and gn with qz gangue. B) Sample 2013-3-3 highlighting sp and cogenetic gn replacing a pyrite grain (or cluster of grains) with grain boundary defined by white dashed line. C) Sample 2013-3-8 highlighting prominent cubic gn hosted in cal. Brighter spots on gn have higher Pb to S ratio. D) Sample 2013-3-10 highlighting cogenetic cpy and gn hosted in cal. E) Sample 2013-3-9 BSE-EDX map highlighting gn crystal growth in fractures and in void space within cpy. Py appears to replace cpy and have mineralised alongside cb and qz gangue. Panel 'e' was created using a series of semi-transparent overlays of the BSE, Fe, Cu, and Pb large area maps from Bruker Esprit software and the final bronze colour of cpy in the figure is due to the mixing of Fe and Cu colours (purple and yellow). Mineral abbreviations: cal = calcite, cb = carbonate mineral, cpy = chalcopyrite, gn = galena, py = pyrite, qz = quartz, sd = siderite, sp = sphalerite (Whitney and Evans, 2010).

Figure 4: Boxplots of log-transformed concentrations of Ge, Ag, and Sb in sphalerite from the LWO compared to that from epithermal, MVT, and stratabound deposits from a global dataset.

Table 1: Element concentrations in galena, chalcopyrite, sphalerite, and pyrite from the Leadhills and Wanlockhead orefield determined by LA-ICP-MS spot analysis. Data in ppm. Blanks indicate below detection limit for the given element. NA = high value/error or typically a main constituent of the mineral.

Table 2: Data for Ga, Ge, In, Sb, and Ag concentrations in the continental crust and ore deposits compared to the Leadhills-Wanlockhead orefield. References in text.

Table 3: Comparison of sphalerite LA-ICP-MS minor and trace element data from Leadhills and Wanlockhead to other deposit styles globally.

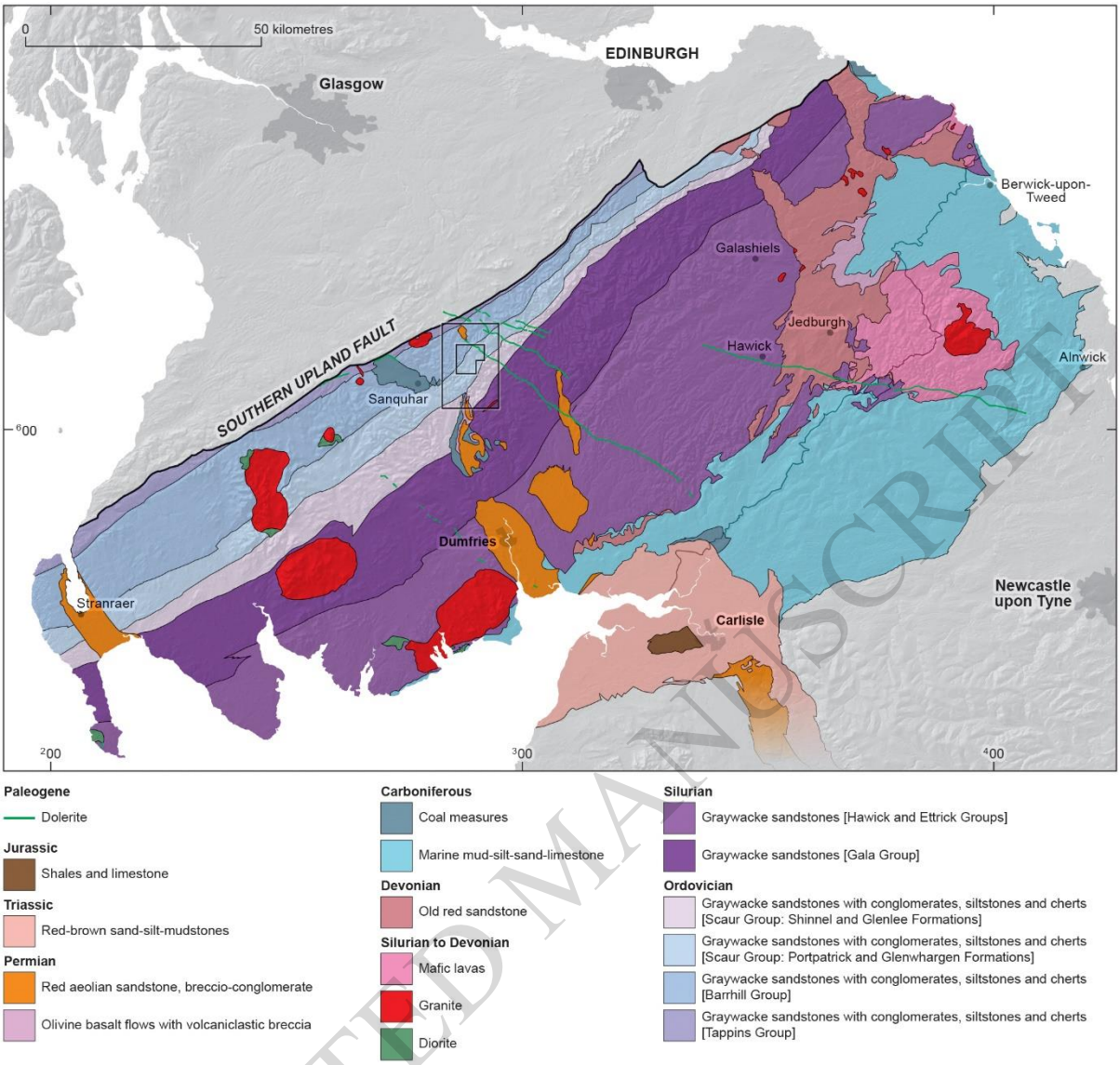

Figure 1a

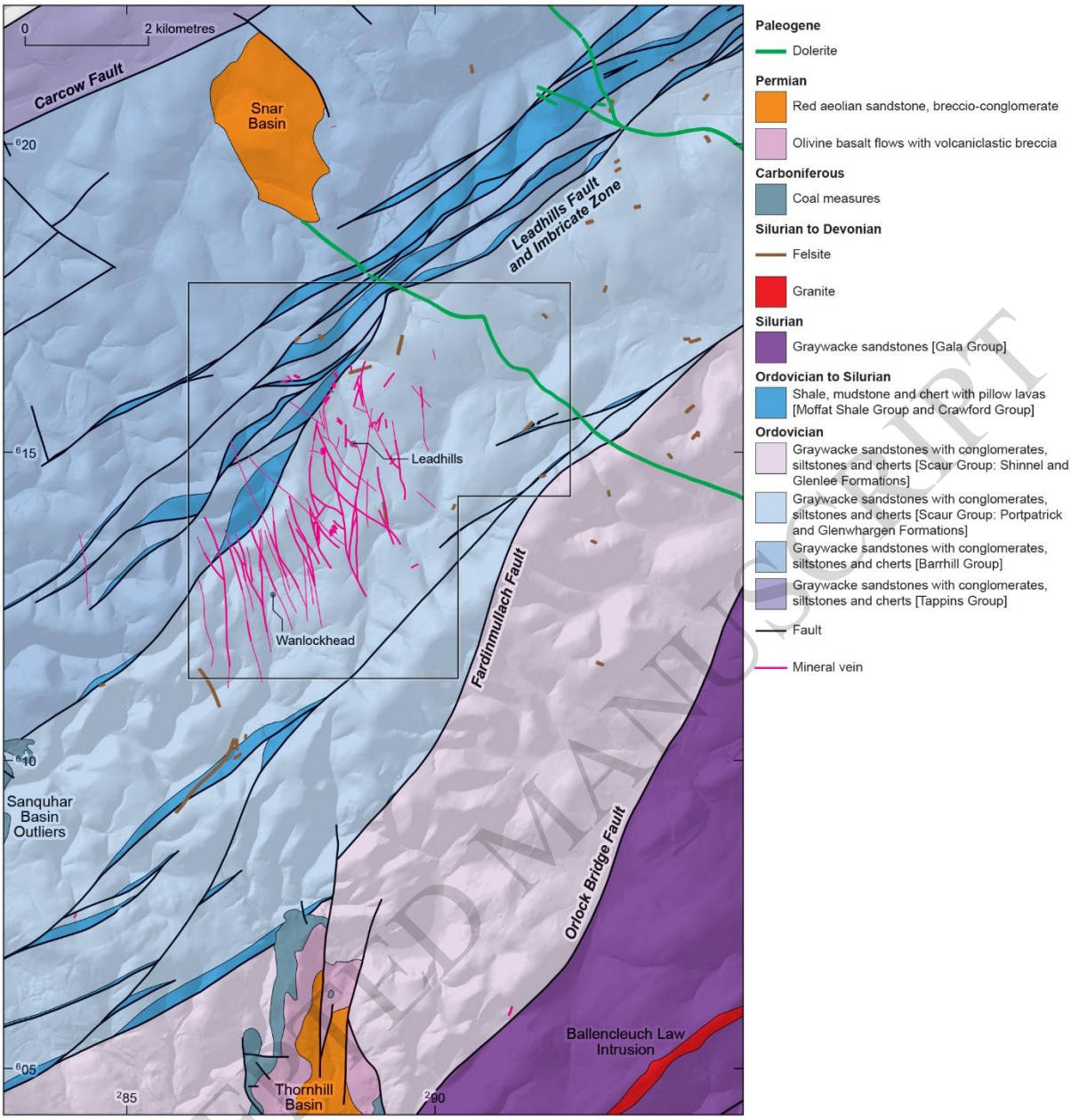

Figure 1b

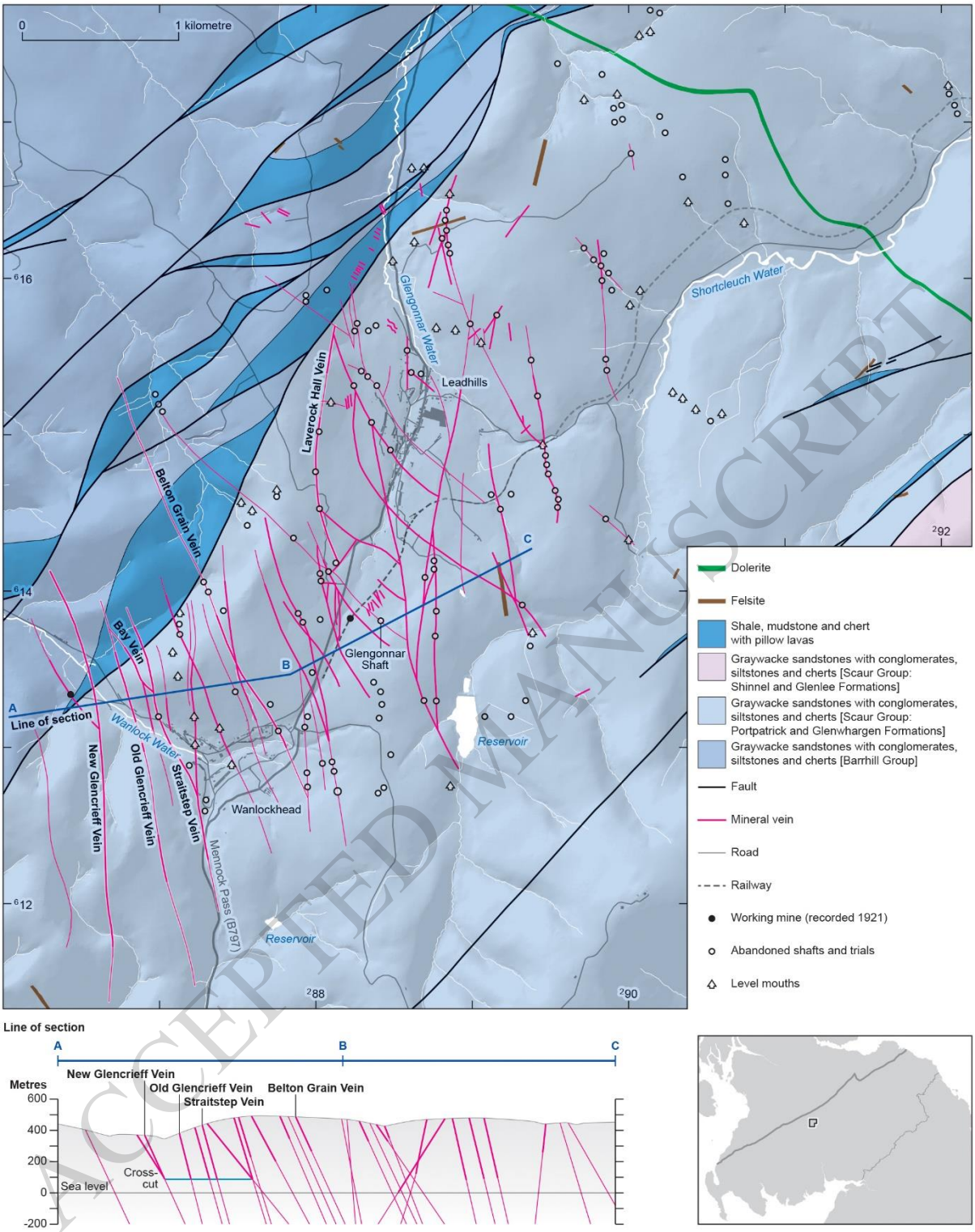

Figure 2

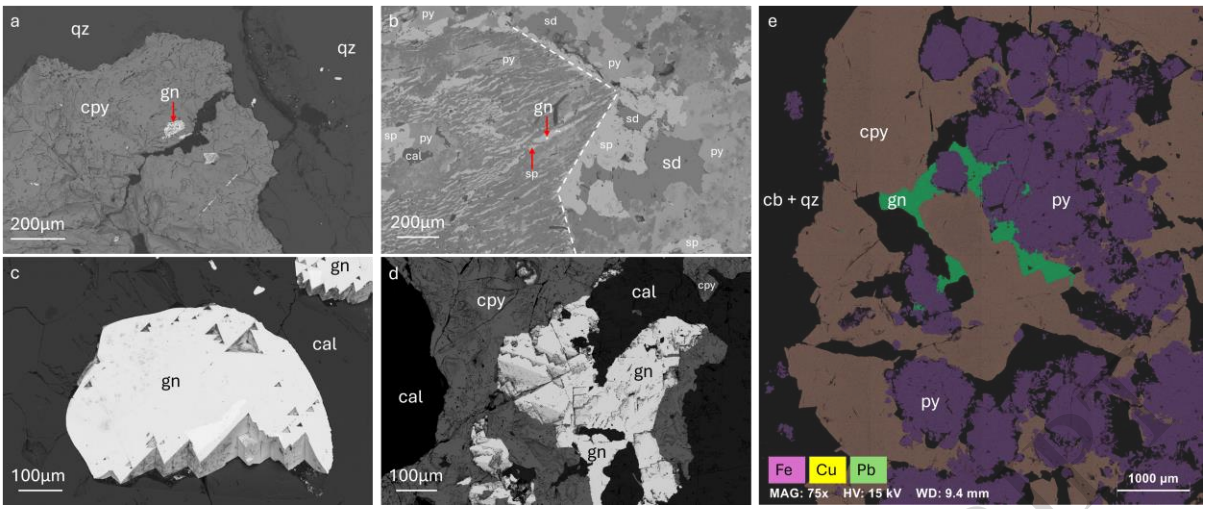

Figure 3

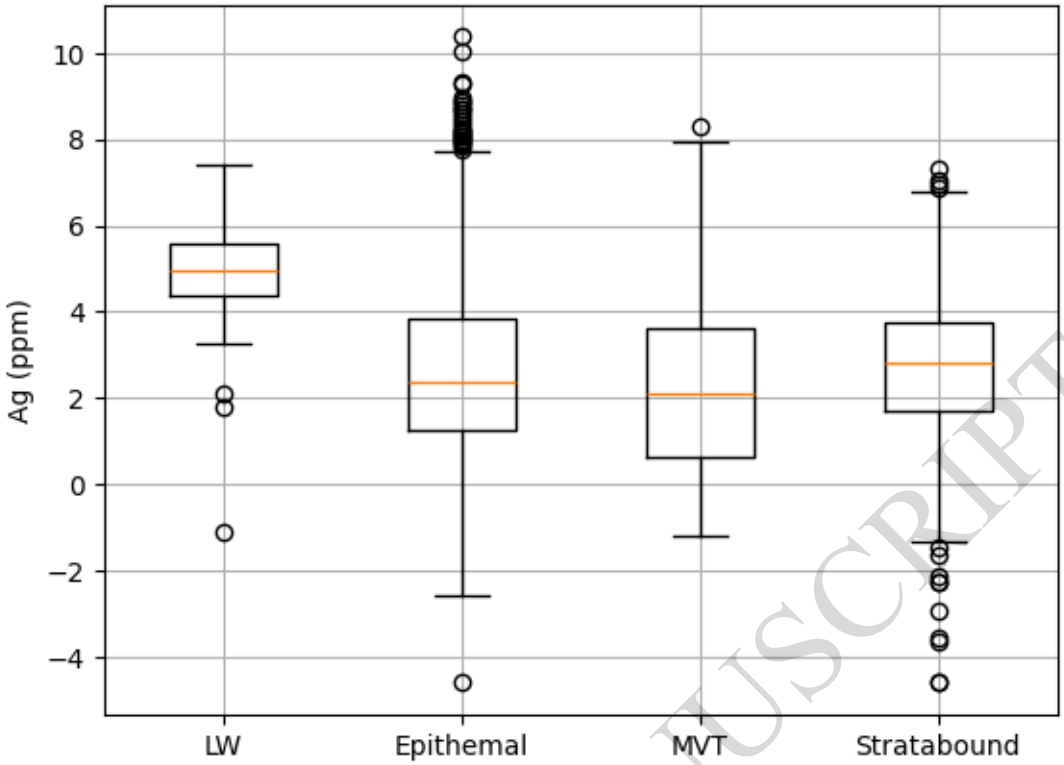

Figure 4a

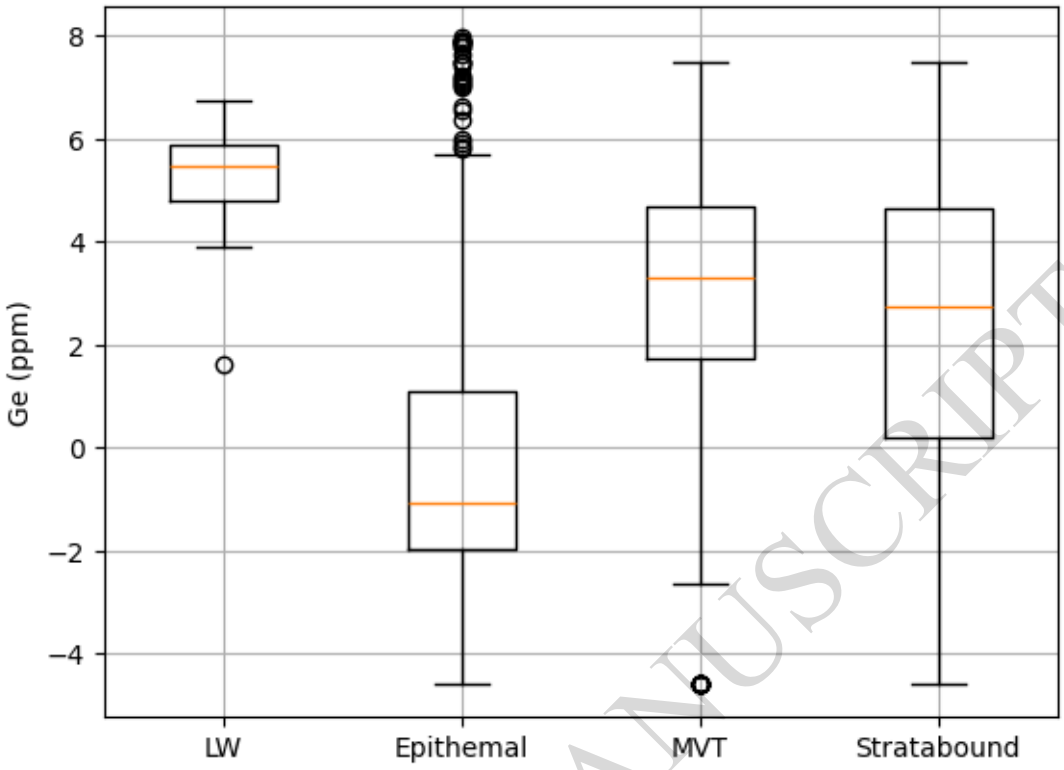

Figure 4b

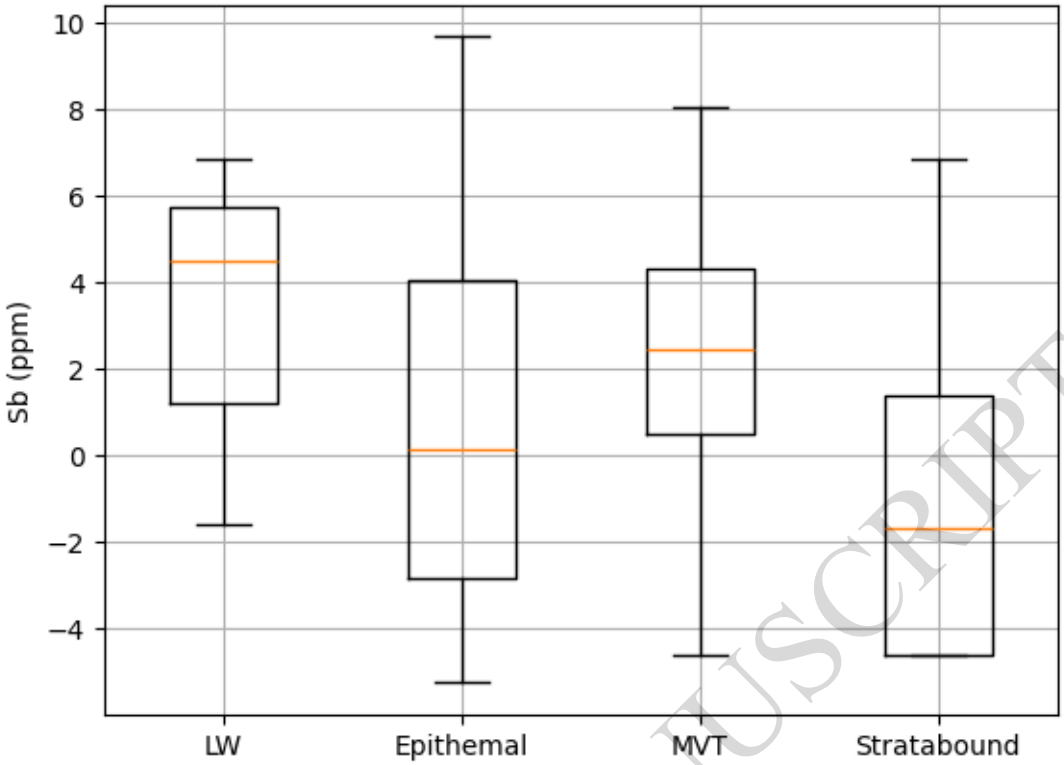

Figure 4c

Table 1: Element concentrations in galena, chalcopyrite, sphalerite, and pyrite from the Leadhills and Wanlockhead orefield determined by LA-ICP-MS spot analysis. Data in ppm. Blanks indicate 'below detection limit for the given element' with values for typical detection limit as table footer. NA = high value/error or typically a main constituent of the mineral.

		Element (concentration in ppm)																	
Sulfide		**Mn**	**Fe**	**Co**	**Ni**	**Cu**	**Zn**	**Ga**	**Ge**	**As**	**Mo**	**Ag**	**Cd**	**In**	**Sn**	**Sb**	**Bi**	**Se**	**Pb**
Galena (54)	GM					0.3						16	2.5			75	0.2	5.4	NA
	error					0.1						1.9	0.7			11	0.04	1.2	NA
	Maximum		5.3		0.9	4.1				5.9		520	10	6.4	11	1300	1.7	40	NA
Chalcopyrite (74)	GM			0.2	0.4	NA	100		2.5	0.5		2.1	1.3	21	21	0.9	0.3	17	NA
	error			0.1	0.8	NA	27		1.5	0.9		0.4	1.6	3.8	9.8	0.6	0.2	7.5	NA
	Maximum	110	NA	5.3	6.0	NA	680	6.3	76	20.2	5.3	100	4.4	150	200	25	66	260	770
Sphalerite (34)	GM	12	24000	2.3		240	NA	6.4	200	1.3		120	2400	0.3	2.2	30			66
	error	2.6	4100	0.4		21	NA	0.9	29	0.7		19	600	0.2	1.5	7.5			8.6
	Maximum	54	100000	14	0.6	1700	NA	140	860	21		1700	5900	70	160	960	1.7	9.1	650
Pyrite (40)	GM	10	NA	1.4	1.7	5.3	8.1			25	0.3	0.1		0.1		1.8		2.6	12
	error	1.8	NA	0.3	0.7	2.6	3.4			6.6						0.4		1.4	2.4
	Maximum	1500	NA	130	160	14000	82	0.1	8.3	12000	17	59	1	29	10	51		58	500
Typical Detection Limit		*0.7*	*2*	*0.002*	*0.3*	*0.2*	*4*	*0.002*	*0.3*	*0.5*	*0.002*	*0.02*	*0.8*	*0.03*	*0.8*	*0.3*	*0.05*	*0.3*	*0.4*

Table 2: Data for Ga, Ge, In, Sb, and Ag concentrations in the continental crust and ore deposits compared to individual minerals from the Leadhills-Wanlockhead orefield. References in text.

Element	Crustal Abundance (ppm)	Mean Ore Deposit Grade (ppm)	Geometric mean LWO (ppm)	Maximum value LWO (ppm)
Ga	17.5	100s to >1000	6.4	140
Ge	1.4	100 to 850	200	860
In	0.056	200 to 300	21	150
Sb	0.4	tens of wt %	75	1300
Ag	53	33 to >600	120	1700
Se	0.09	240 to 640	17	260

Table 3: Comparison of sphalerite LA-ICP-MS minor and trace element data from Leadhills and Wanlockhead to other deposit styles globally.

		Element (concentration in ppm)							
Deposit type (data points)		**Cd**	**Cu**	**Ga**	**Ge**	**In**	**Sb**	**Sn**	**Ag**
Leadhills-Wanlockhead (n=34)	*GM*	2400	240	6.4	200	0.3	29	2.2	120
	Max	5900	1700	140	860	69	960	160	1700
Skarn (n=264)	*GM*	3900	95	0.7	0.5	7.5	0.2	0.4	5.7
	Max	130000	25000	170	48	4000	1200	440	360
Frenzel et al. (2016) - HTHR	*GM*	2900	140	3.1	1.4	16	NA	NA	15
Epithermal (n=1027)	*GM*	2500	300	13	0.5	9	2.3	10	15
	Max	21000	65000	2100	2900	67000	16000	34000	32000
Frenzel et al. (2016) - Vein	*GM*	3200	690	14	5	14	NA	NA	42
Stratabound (n=266)	*GM*	1700	40	0.4	7.4	NA	0.2	0.2	15
	Max	7900	4900	280	1200	52	570	78	1500
SHMS-VHMS (n=322)	*GM*	5000	97	11	0.6	6.3	0.7	0.8	7.4
	Max	9600	14000	860	23	570	120000	3100	2800
Frenzel et al. (2016) - SHMS	*GM*	2400	310	11	3.7	10	NA	NA	16
Frenzel et al. (2016) - VHMS	*GM*	2100	1100	19	2.2	22	NA	NA	13
MVT (n=674)	*GM*	2400	48	5.0	20	NA	8	0.6	9.6
	Max	69000	15000	1300	1100	20	3100	74	4000
Frenzel et al. (2016) - MVT	*GM*	3600	350	42	63	2.2	NA	NA	12